Selection of Hydrofoil Waterjet Propulsion Systems

ROSS HATTE* AND HUGH J. DAVIS†
The Boeing Company, Seattle, Wash.

The selection of waterjet propulsion systems for hydrofoil craft requires sophisticated techniques which must take into account the mutual interaction of numerous craft subsystems. These interactions include the effect of parasitic (appendage) drag, cruise and takeoff power levels, subsystem weight fractions, and machinery room arrangements. It is shown that propulsive efficiency, per se, is not a useful parameter as a selection yardstick even when rigorously evaluated to account properly for all internal duct losses. The recommended selection technique consists of the comparative evaluation of over-all craft performance for numerous integrated subsystem combinations by means of a comprehensive digital computer program. It is shown by a specific example, i.e., a 300-ton, 50-knot hydrofoil craft, that through the recommended approach and the use of state-of-the-art pumps with proven design features, power requirements and total waterjet-system weight fractions can be maintained at reasonable levels. This objective is achieved without resorting to more sophisticated pump designs which normally require state-of-the-art verification for application to waterjet propulsion. Also included is a discussion of the critical elements of waterjet subsystems, with particular emphasis on the technique required for the experimental evaluation of suitable inlet configurations.

Nomenclature

η = actual propulsive efficiency, or the ratio of the craft power consumption to the prime-mover output-shaft power, $(V_1)(D)/550$ BHP
$\bar{\eta}$ = η divided by pump and speed-converter efficiencies
$\bar{\eta}_i$ = ideal propulsive efficiency (no inboard losses), $2/(r_o + 1)$
V_2 = nozzle jet velocity, fps
V_1 = craft velocity, fps
V^k = craft velocity, knots
r = ratio of nozzle-jet velocity (with respect to craft) to craft velocity
D = total craft drag, lb
H_L = sum of all inboard losses excluding pump, speed-converter, and prime-mover losses, ft
K_A, K_B = inboard loss coefficients [Eqs. (2–7)]
K_2 = nozzle head loss coefficient [Eqs. (8–10)]
DLF = "duct-loss-factor." This term incorporates all of the individual geometric terms of the total duct, the associated fluid-mechanics terms, and a non-dimensional drag term to reflect the variations in power-strut/pod parasitic drag [Eqs. (8–10)]
g = gravitational constant, ft/sec^2
R = craft range, naut miles
W_f = available propulsion fuel, lb
SFC = prime-mover, specific fuel consumption, lb per BHP-hr
GW = L = design gross weight of craft, lb
A = weight fraction of total waterjet system (W_f not included)
B = weight fraction of all items making up gross weight exclusive of waterjet system and available propulsion fuel [fixed quantity in Eq. (12)]
PL = design payload, lbs (W_f not included)
C = weight fractions of all items making up gross weight exclusive of waterjet system, payload, and available propulsion fuel [fixed quantity in Eq. (13)]
BHP = prime-mover output-shaft horsepower, ft-lb/sec
M = design thrust-to-drag ratio at takeoff-drag hump
Y = fuel economy parameter, $(PL)(R)/W_f$
N_s = pump specific speed. This parameter characterizes the impeller flow/head/rpm relationship. (Discharge is expressed in gal/min units per impeller side. Other units are ft and rpm.)
N_{su} = pump suction specific speed. This parameter characterizes the impeller resistance to cavitation. (Discharge is expressed in gal/min units per impeller side. Other units are ft and rpm.)
σ_c = critical cavitation sigma
$(NPSH)_c$ = minimum required energy level (above vapor pressure) at the pump inlet, ft
H_p = pump head, ft
σ_i = Thoma cavitation index
H = any convenient energy head in the model, such as a velocity head, ft
ΔH = available static pressure above water vapor pressure, ft

Subscripts denoting operational mode

o = design foil-borne mode
to = takeoff mode at the drag hump

Presented as Preprint 66-732 at the AIAA/USN 2nd Marine Systems & ASW Conference, Los Angeles-Long Beach, Calif., August 8–10, 1966; submitted August 8, 1966; revision received February 20, 1967. [4.22, 5.08, 6.14]

* Chief, Performance Staff, Advanced Marine Systems, Aerospace Group.
† Design Specialist, Advanced Marine Systems, Aerospace Group. Member AIAA.

I. Introduction

THE hydrofoil is a unique marine vehicle in which the technology of flight is combined with that of traditional naval architecture. Because it is a composite vehicle, its success or failure is unusually sensitive to the details of its design. Since the craft must fly as well as withstand the rigors of the sea, its structure tends to be heavier than its flying cousin, the airplane. Thus, the available weight fraction for fuel is always found to be small, of the order of 20% of the craft weight. Consequently, the propulsion system selected for the craft must be lightweight as well as efficient in its use of fuel if reasonable range or payload performance is to be obtained. However, the craft performance is not only a function of the waterjet internal performance but also of its external performance. That is, the parasitic drag and the total weight of the waterjet system, including the contained water weight, must be considered in design studies. Because of this mutual interaction, the design of the most suitable propulsion system is more complex than in conventional craft where this situation does not normally exist. This paper will describe the methods developed for waterjet propulsion system selection by the Boeing Company since 1961, in addition to some of the more salient aspects of the developmental work in support of this endeavor.

II. Discussion

A. Waterjet System

1. *Components*

Figure 1 shows a schematic representation of a typical waterjet system for hydrofoil craft application. The system comprises three primary elements: the inlet system, the pump, and the outlet system. The inlet system is normally contained in one or more of the struts that support the foils. It comprises an inlet scoop, containing a 90° elbow, a vertical duct in the strut, and a transition duct to the pump inlet flange. The design of the inlet system is found to be of critical importance to the propulsion system design. It is usually characterized by low internal losses and high resistance to cavitation during the takeoff mode and by low external drag during cruise. The pump may be of axial-flow, mixed-flow, or centrifugal-flow design. This component is usually characterized by high efficiency, light weight, small size, and high resistance to cavitation. The outlet system may incorporate nozzles of either fixed or variable geometry, depending on the specific craft requirements. These nozzles are also usually of high efficiency and lightweight design.

2. *Energy breakdown*

The concept of a hydrofoil waterjet propulsion system is unique in the respect that, for the practical case, relatively long, high-velocity ducts are required between the inlet and outlet sections of the system. For this reason, in the selection of this type of system, careful attention must be given to the internal and external dissipation of fluid energy which results from the choice of design flow rate and internal duct design. Figure 2 is presented to emphasize the wide differences in characteristics inherent in the waterjet concept. This figure displays the energy breakdown for systems incorporating identical internal duct configurations, but representing two separate values of jet-velocity ratio (r_o = 2.5 and r_o = 1.5). Both systems are designed to produce the identical thrust at the same design speed. The indicated wide differences in system internal losses, jet residual loss, and useful propulsion energy show the importance of the jet-velocity-ratio parameter as a design tool.

B. Propulsive Efficiency

Early in the hydrofoil program, general studies of selected propulsion systems were made to obtain comparisons of craft performance. Based solely on the criterion of propulsive efficiency, it was demonstrated that hydrofoil craft driven by propellers appeared to out-perform waterjet-driven craft at all speeds under consideration. The results of this early study are summarized in Fig. 3.

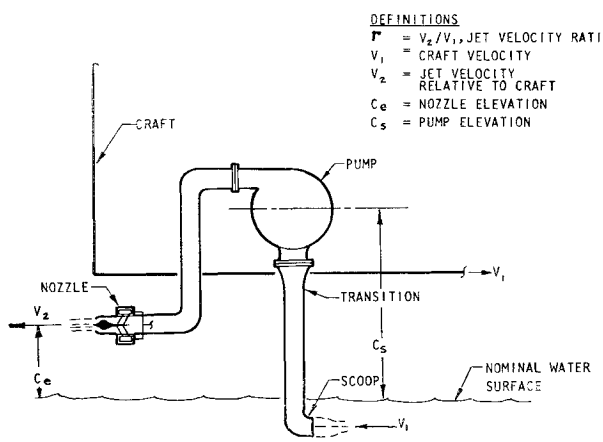

Fig. 1 Waterjet schematic.

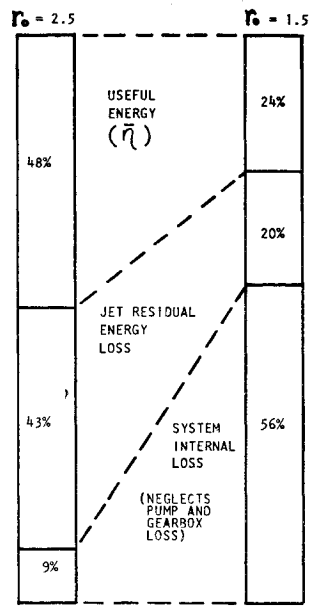

Fig. 2 Waterjet energy breakdown.

However, Fig. 3 is misleading in the following two respects.

1) It does not provide an adequate yardstick for propulsion system selection. As more detailed knowledge of the characteristics of hydrofoil propulsion systems was acquired, it became evident that propulsive efficiency, per se, could not be used to measure the desirability of a particular system, or to make comparison of basic propulsion types. For waterjet systems it was consistently found that a higher propulsive efficiency actually would result in lower over-all system performance because of the effects of parasitic drag and waterjet-system weight fractions. The discussions that follow demonstrate the inadequacy of propulsive efficiency as a reliable design tool for the selection of waterjet system parameters and how, rather than being used as a major design input, propulsive efficiency is relegated to the role of an interesting by-product of the design process.

2) The band of waterjet-system propulsive efficiencies shown in Fig. 3 does not properly incorporate the full range of potential efficiencies associated with this type of system. The full range of these potential (but from an over-all performance criterion, not necessarily desirable) efficiencies which can be achieved by waterjet systems, and the parameters that are related to these efficiencies, are discussed in Sec. IIB1 which follows.

1. *Variation in concepts*

Numerous authors have shown that propulsive efficiency is dependent on the ratio of the nozzle outlet velocity to the craft velocity. Concurrence exists for the algebraic expression of the "ideal" propulsive efficiency, i.e., the expression for no inboard losses:

$$\bar{\eta}_i = 2/(r_o + 1) \qquad (1)$$

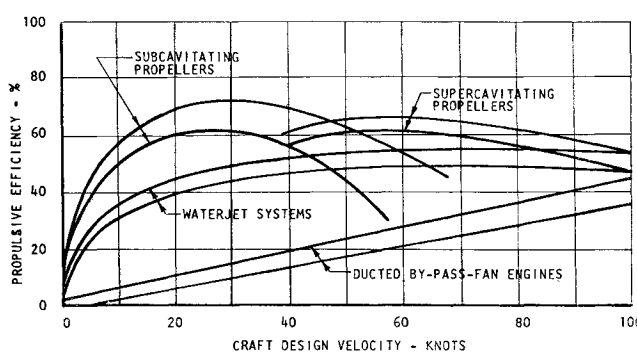

Fig. 3 Generalized efficiency of selected systems.

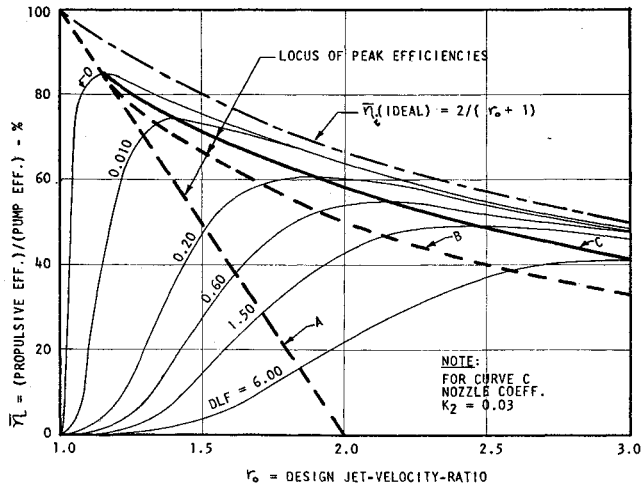

Fig. 4 Locus of optimums.

where $\bar{\eta}_i$ is the ideal propulsive efficiency and r_o is the ratio of the jet velocity (referred to the craft) to the craft velocity.

It is also generally accepted that $\bar{\eta}_i$ is not useful in defining the performance of an actual system since the effects of the inboard energy losses are normally of major significance. For this reason, most authors derive an expression that reflects the efficiency of an actual waterjet system ($\bar{\eta}$) which accounts for various degrees of internal duct and nozzle losses, but which ordinarily does not include the energy losses in the pump. This treatment is logical because pump efficiency is not normally a function of jet velocity ratio, and because the pump efficiency factor can be readily incorporated in the final calculation when the pump details are known.

Most authors, however, adopt independent methods for incorporating the duct and nozzle losses in the propulsive efficiency derivation. Unfortunately, these independent methods result in a surprising variance in the mathematical expressions, and the associated $\bar{\eta}$ vs r_o (or equivalent) design curves which are often used in the waterjet selection process. The use of these design curves often leads to widely inconsistent waterjet-system selection in spite of the fact that such curves evidently are intended to assist in defining the most suitable waterjet system for a particular hydrofoil mission. Figures 4 and 5 have been prepared to clarify this inconsistency.

Figure 4 is primarily a plot of a family of $\bar{\eta}$ vs r_o curves, where $\bar{\eta}$ is the ratio of actual propulsive efficiency (η) divided by the pump efficiency. The actual propulsive efficiency is defined as the ratio of the craft power consumption (product of speed and total craft drag) to the prime-mover output-shaft power. In this definition, the waterjet-system parasitic drag is included in the total drag term. In addition, in the event that a speed converter is required between prime mover and pump, the additional loss factor is incorporated in the pump-efficiency term.

Also shown in Fig. 4 are three heavy lines designated A, B, and C, representing the locus of peak efficiencies calculated by the three independent methods discussed below. Note that the individual $\bar{\eta}$ vs r_o curves shown are only those associated with curve C (i.e., those which peak on curve C). For clarity, the individual $\bar{\eta}$ curves peaking on A and B are omitted and may be obtained from Refs. 1 and 2.

Curve A is based on a recent paper[1] where all inboard losses are expressed as a direct function of the nozzle jet velocity head

$$H_L = K_A \cdot V_2^2/2g \tag{2}$$

and the corresponding propulsive efficiency as:

$$\bar{\eta} = 2(r_o - 1)/[r_o^2(1 + K_A) - 1] \tag{3}$$

The resulting expression for curve A, obtained by equating the first derivative of Eq. (3) to zero, is

$$r_{\text{peak}} = [K_A/(1 + K_A)]^{1/2} + 1 \tag{4}$$

In the preceding equations, H_L represents the sum of the duct and nozzle losses; K_A is a loss coefficient, and V_2 is the nozzle jet velocity. The nozzle elevation loss is neglected.

For a given mission and a particular craft configuration, the speed and thrust requirements are evidently fixed. In addition, the waterjet-system flow rate, defined by the momentum relation, will vary inversely with $(r_o - 1)$, and V_2 obviously will vary directly with r_o. Consequently, the premise for curve A that the duct and nozzle losses vary directly with $V_2^2/2g$ actually is imposing the arbitrary, and usually unrealistic, requirement that the duct areas, as well as the nozzle area, must vary inversely with $r_o(r_o - 1)$ for each individual $\bar{\eta}$ vs r_o curve. The parasitic-drag variations, in turn, cause variation in the required system flow rate and associated power requirements, both of which are neglected.

Curve B is based on another recent paper[2] in which the duct, nozzle, and nozzle elevation losses are expressed, this time as a function of the craft velocity head

$$H_L = K_B \cdot V_1^2/2g \tag{5}$$

and the corresponding propulsive efficiency as

$$\bar{\eta} = 2(r_o - 1)/(r_o^2 - 1 + K_B) \tag{6}$$

The expression for curve B, obtained in the same manner as for curve A is

$$r_{\text{peak}} = [K_B + 2(K_B)^{1/2} + 1]^{1/2} \tag{7}$$

In this case the locus of the peaks of the individual $\bar{\eta}$ vs r_o curves is not limited to r_{peak} smaller than 2 (as for A), but can have significantly larger values with no mathematical limit. In Eqs. (5–7), H_L represents the sum of the duct, nozzle, and nozzle elevation losses; K_B is another loss coefficient which includes the nozzle elevation factor; and V_1 is the craft design velocity.

As mentioned under the discussion for curve A, for a given mission and a particular craft configuration, the speed and thrust requirements are fixed. For curve B, however, since the internal losses are assumed proportional to the craft velocity head, these losses are constant, and the duct velocities are essentially constant, as r_o varies. As discussed for curve A, the flow rate varies inversely with $(r_o - 1)$. Consequently the internal-loss premise for curve B again imposes an arbitrary requirement, this time that duct areas vary essentially inversely with $(r_o - 1)$, also without regard to the parasitic-drag variations (as readily admitted by the author).

Curve C is based on a comprehensive and detailed propulsive efficiency expression derived by one of the co-authors in 1961. The basis of this expression has been used since that time as part of a versatile digital computer program for evaluating numerous waterjet-system applications (see Sec. III).

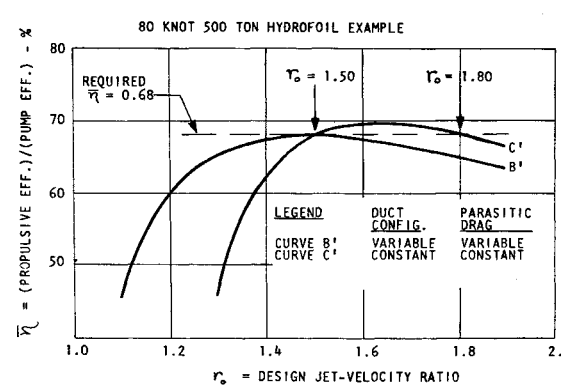

Fig. 5 Comparison of two methods.

In contrast to the methods represented by curves A and B, curve C is based on an approach where the inboard losses are not lumped in a single category, and are not made proportional to either the nozzle-jet or craft-velocity heads, a constraint which is not considered realistic. The nozzle, duct, and elevation head losses are treated as separate entities which are varied independently, and which are made to reflect changes in flow rate resulting from variation in power-strut and inlet-pod parasitic drag. Consequently the duct loss terms K_2 and DLF in the equations below include a dimensionless drag term, as well as dimensionless terms which reflect individual duct component areas, lengths, hydraulic radii, skin roughness, turning, and nozzle-elevation losses. The three basic expressions which substantiate curve C, greatly condensed to facilitate comparison with Eqs. (2–7), are

$$H_L = \left[K_2 r_o^2 + \left(\frac{1}{r_o - 1}\right)^2 (\mathrm{DLF})\right]\frac{V_1^2}{2g} \tag{8}$$

$$\bar{\eta} = \frac{2(r_o - 1)}{r_o^2(1 + K_2) - 1 + \left(\frac{1}{r_o - 1}\right)^2 (\mathrm{DLF})} \tag{9}$$

$$r_{\mathrm{peak}} = 1 + \left\{\frac{K_2 + [K_2^2 + 12(1 + K_2)(\mathrm{DLF})]^{1/2}}{2(1 + K_2)}\right\}^{1/2} \tag{10}$$

In contrast to curves A and B, curve C does not impose the constraint resulting in an arbitrary variation in duct geometry for each of the $\bar{\eta}$ vs r_o family of curves. On the contrary, the curve C approach allows the investigation of a family of craft configurations where both the duct sizes and total craft drag are held fixed for each particular craft configuration.

It is evident from Fig. 4 that the use of propulsive-efficiency design curves of the type analyzed will yield significantly different solutions. To indicate the magnitude of such differences, an example is discussed below.

2. *Variations in selection—specific example*

In this example a waterjet system is to be chosen for an 80-knot, 500-ton hydrofoil.[2] The cruise and takeoff power available are fixed at 120,000 and 180,000 BHP, respectively. The cruise and takeoff thrust required are also fixed at 300,000 and 400,000 lb, which, in turn, essentially fix the waterjet parasitic drag. From these data, and for an assumed pump efficiency of 90%, the "required" $\bar{\eta}$ is calculated as 68%. Concurrently it must also be assumed that the inlet-duct design compatible with the craft parasitic-drag requirement will also provide the relatively high propulsive efficiency required. As discussed in Ref. 2, an $\bar{\eta}$ vs r_o design curve was chosen (actually $\bar{\eta}$ vs H^*, where $H^* = r_o^2 - 1 + K_B$) which peaks at 68% for an r_o value of 1.50. This curve is shown on Fig. 5 as curve B′, and is calculated using Eq. (6). Using the identical duct and nozzle design as for curve B′, curve C′ has been calculated, using Eq. (9), to pass through the design point of curve B′. It is noted, however, that curve C′ peaks to the right, and recrosses the required $\bar{\eta} = 68\%$ for an r_o value of 1.80, a significant improvement in design as will now be shown.

Separate detailed performance calculations for the identical 500-ton hydrofoil craft described previously have been made using both curves B′ and C′ as design tools for the selection of the waterjet system. The identical mission and over-all craft requirements specified previously are applicable to both sets of calculations. The craft configurations, including the ducts and nozzles, are also identical. The only departure in hardware configurations is in the pumps and speed converters which are made compatible with the respective design values of jet-velocity ratio ($r_o = 1.50$ vs $r_o = 1.80$). In this connection, it should also be noted that the same number, arrangement, and basic type of pumps (i.e., conventional designs with the same specific speed) are used for each alternative, the essential difference being the rpm and size factors, and the associated flows and heads.

Predicated on the use of curves B′ and C′ and the constraints described previously, the following changes in the waterjet system characteristics have been calculated. The designated changes apply to the use of $r_o = 1.80$ as contrasted to the use of $r_o = 1.50$:

1) The cruise discharge is reduced from 2220 to 1390 ft³/sec, a 37% reduction.

2) The cruise pump head is increased from 420 to 665 ft, a 58% increase.

3) The cruise pump rpm, for the same impeller specific speed, is increased from 1560 to 2780 rpm, a 78% increase.

4) The cruise engine power requirement is identical for both designs.

5) The takeoff engine power requirement is reduced from 151,500 to 117,000 BHP, a 23% reduction. This results from the capability of operating the pump at best efficiency (90%) vs the requirement to throttle the pump at takeoff, under which condition the pump efficiency is reduced to 75%. Note that flow throttling at takeoff is required for the $r_o = 1.50$ high-flow design in order not to exceed the pump cavitation characteristics.

6) The total weight of the waterjet system plus speed converters is reduced from 150 to 83 tons, a weight reduction of 45%. The corresponding over-all weight fraction is thereby reduced from 30% to a more reasonable 16.6%.

3. *Conclusions*

It is concluded from the foregoing analyses that propulsive-efficiency design curves can be misleading when used for the selection of desired waterjet-system parameters. These curves will be misleading unless they represent expressions that incorporate enough detailed terms to account independently for the energy losses in each component element of the system. These loss terms must not be lumped together, and not only must include the geometric factors associated with the flow paths, but also must reflect the effect of parasitic drag on the required flow rate.

Based on numerous other analyses, it is also concluded that even at best, propulsive efficiency is not a suitable criterion for the selection of the most desirable waterjet system for a given craft mission. This conclusion has been reached as a result of many digital computer trades performed by the Boeing Company on a variety of hydrofoil craft. The next section describes the recommended over-all craft criteria that are deemed suitable for this purpose.

Another recent report,[3] based on a selection procedure that again departs from the three already discussed, concurs in regard to the use of over-all craft criteria rather than propulsive efficiency as normally defined. The basic departure in this instance is the use of simplifying coefficients to obtain component weight fractions for evaluation of the craft range and payload criteria. This oversimplification (such as the assumption that pump weights are proportional to the shaft horsepower) is not considered realistic and therefore will also affect the validity of the conclusion regarding the most suitable design selection. (See Section IID3 for a discussion of pump weight fractions.)

C. Criteria Recommended for Waterjet-System Selection

Since propulsive efficiency evidently can be a misleading criterion in determining the best waterjet system, more applicable criteria are required. First, it must be assumed that certain items pertaining to the craft mission are known. These are cruise speed and desired payload or range. If payload is fixed, then range will be variable and will become a criterion for evaluation. On the other hand, if range is fixed, the resulting variable payload will become the criterion.

Another yardstick is the efficient use of power. It is evident that maximizing gross weight for a given power, or minimizing power for a given gross weight, is desirable. In addition, both cruise and takeoff power requirements must be examined in obtaining a balanced design. Finally, the efficient use of fuel to transport a given payload must be considered, particularly in a commercial operation, as an additional over-all craft criterion.

Other criteria less amenable to analytical evaluation, such as mechanical reliability, first cost, maintenance costs, and operational life, are also considered of major importance in influencing the final waterjet design. However, these criteria are outside the scope of this paper, and consequently the discussion that follows will be limited to payload, range, power, and fuel economy.

1. *Range and payload*

In developing the over-all vehicle criteria, the following parameters are considered fixed for a particular analysis: design gross weight GW, design cruise speed V_o^k, and design payload PL or range R. In short, the objective is the design of a craft of a given size for a specific mission. The mission may be defined in the following alternative terms depending on the particular requirement:

1) To transport a given payload at a given speed. This requirement implies a variable range which thus becomes one of the desired criteria.

2) To cruise for a required distance at a given speed. This requirement implies a variable payload which thus replaces range as one of the desired criteria.

One of the inherent characteristics of hydrofoils is that foil-borne drag is unusually sensitive to the craft configuration below the flying waterline. Alternative propulsion schemes that are associated with varying parasitic drag consequently result in variable lift-to-drag ratios L/D. In addition, for a fixed gross weight, any change in the propulsion-system weight will be reflected either in a variation in the loaded fuel weight and the associated range, or in the payload. The specific relations between these and other parameters that affect range and payload are discussed in the following two subsections.

a) Range criterion (fixed payload case): The range equation for a hydrofoil may be written as

$$R = 326 \frac{(\eta)(W_f)}{(D)(\mathrm{SFC})} \tag{11}$$

To express range in nondimensional terms, Eq. (11) may be rewritten as

$$R = 326 \left[\frac{(\eta)(L/D)}{\mathrm{SFC}}\right][1 - (A + B)] \tag{12}$$

where $[1 - (A + B)] = W_f/\mathrm{GW}$ = weight fraction of available propulsion fuel.

It is seen from Eq. (12) that the five range parameters do not influence range in the same degree. As an example, it may be assumed for simplicity that an improvement in η is associated with no change in L/D or SFC, but only an increase in A. For this assumption, it is evident that the variation in range will be directly proportional to the change in η, but influenced by A in a more complex manner: If in the chosen example the fuel weight fraction $[1 - (A + B)]$ is small, a relatively small increase in A will result in a relatively large reduction in range, and the converse naturally applies. The net effect of changes in these two variables therefore can result in an increased or reduced range performance, depending on the specific craft under consideration. In an actual situation, the problem is compounded by the fact that a change in the propulsion system is usually accompanied by a change in L/D as well, resulting from a variation in parasitic drag.

b) Payload criterion (fixed range case): An analysis similar to the preceding one results in an expression for payload fraction in the following nondimensional terms:

$$\frac{PL}{\mathrm{GW}} = 1 - \left[A + C + \frac{(R)(\mathrm{SFC})}{(326)(L/D)(\eta)}\right] \tag{13}$$

where

$$\left[\frac{(R)(\mathrm{SFC})}{(326)(L/D)(\eta)}\right] = \frac{W_f}{\mathrm{GW}} = \text{weight fraction of available fuel}$$

By comparing Eqs. (12) and (13), it is seen that the same five variables influence both the range and payload fraction criteria. However, the variables in the two equations are related in a different manner (for example, η affects range directly but affects payload fraction in a smaller degree), and the Boeing Company computer design trades have shown that the choice of fixed range or fixed payload in defining the hydrofoil mission has a demonstrable effect on the selection of the most suitable system.

2. *Power*

In addition to range, the required cruise and takeoff power must be determined as part of the performance evaluation. The relationship between required power at design cruise and at the takeoff-drag hump may vary significantly between alternate designs of propulsion systems, as well as alternate designs of other subsystems such as the hull, foils, and struts. Takeoff power may be higher, equal, or lower than cruise power depending on the net effect of the following four factors: 1) drag relationship at cruise and takeoff, 2) speed relationship at cruise and takeoff, 3) propulsive-efficiency relationship at cruise and takeoff, and 4) design thrust-over-drag margin at takeoff.

The expressions for cruise power and takeoff power are as follows:

$$\mathrm{BHP}_o = \frac{(V_o^k)(D_o)}{(326)(\eta_o)} \tag{14}$$

$$\mathrm{BHP}_{to} = M \frac{(V_{to}^k)(D_{to})}{(326)(\eta_{to})} \tag{15}$$

For a given gross weight, hull, and foil system design, V_{to} and D_{to} are essentially constant since the effects on takeoff drag of the waterjet system configuration are minor. In addition the thrust-to-drag ratio at takeoff, M, is usually fixed during the initial design stage in order to assure a satisfactory takeoff margin. Therefore power requirements at cruise and takeoff, as affected by the choice of the waterjet system, are influenced by three variables, i.e., D_o, η_o, and η_{to}, or actually D_o, η_o, and r_o, since η_{to}/η_o is primarily a function of r_o, as indicated in Sec. IID3.

3. *Fuel economy*

Another criterion which can be useful in evaluation of the craft performance, particularly for commercial application, is its fuel economy expressed as ton-miles of payload per ton of consumed fuel. Thus fuel economy Y may be written

$$Y = (PL)(R)/W_f \tag{16}$$

Since the fuel-economy criterion incorporates parameters already treated in the preceding sections, the foregoing discussion of the interrelation of the parameters applies here also.

D. System Design Selection

Section IIC discusses the recommended system-selection criteria, and the relationship of these criteria to certain key subsystem parameters. The present section discusses the

manner in which the craft systems and subsystems mutually interact, and the means by which this complex interaction may be evaluated realistically. Following this, a typical example is discussed which summarizes the results of the recommended technique.

1. *System performance interaction*

As described in Sec. IIA, a waterjet propulsion system incorporates components that are physically integrated into the vehicle configuration which, in turn, results in a complex mutual interaction. From the propulsion-design standpoint, the waterjet performance is unusually responsive to the geometry and performance characteristics of individual craft components including the hull, the struts and foils, and the machinery space allocation. The following areas of interaction are listed below and are illustrated in Fig. 6, which is a schematic representation of this mutual interplay: 1) inlet-scoop design and resulting inlet-duct geometry, with associated effect on pump-cavitation limits and propulsive efficiency; 2) strut design and resulting over-all duct geometry, with associated effect on pump cavitation, propulsive efficiency, and system weight; 3) hull design and resulting takeoff-hump drag and over-all outlet-duct and nozzle geometry, with associated effect on propulsive efficiency and system weight; 4) foil design and resulting characteristics of over-all drag curve; and 5) over-all vehicle design and resulting pump and nozzle elevation above the water surface, with associated effect on head, pump cavitation, and system weight.

From the over-all design standpoint, the craft performance is also unusually sensitive to the following waterjet system design choices which either directly or indirectly influence range or payload and required propulsion power: 1) type and size of the inlet scoop, and the resulting effect on drag, foil performance, and takeoff margin (see Fig. 6); 2) size and geometry of the inlet vertical duct, and the resulting effect on the power-strut design, drag, weight fractions, and takeoff margin (see Fig. 6); 3) size and geometry of the outlet duct, and the resulting effect on weight fractions and machinery space arrangement; 4) type and size of propulsion pump and the resulting effect on weight fractions and machinery space arrangement; 5) pump specific speed and suction specific speed, and the resulting effect on takeoff margin (see Fig. 6); 6) pump efficiency and the resulting effect on range and required power; 7) nozzle efficiency and the resulting effect on range and required power; and 8) jet-velocity ratio and the resulting effect on flow rate, parasitic drag, range, and required power.

2. *Digital computer design trades*

The mutual interaction described previously between the over-all performance of the craft and individual component parameters indicates the essential requirement to evaluate many possible design combinations to achieve a good final design. Early design analyses demonstrated that performance optimization of individual subsystem components invariably resulted in relatively poor over-all craft performance. This condition created a need to examine a large number of over-all craft-performance parameters resulting from the many ship subsystem combinations incorporating various degrees of subsystem compromise. A comprehensive digital computer program was therefore conceived and implemented to eliminate the tedious manual calculations required to perform the numerous and complex subsystem performance trades. Since the inception of this effort, more than 1000 waterjet-propelled hydrofoil-craft design variations have been analyzed with this digital tool. Although the bulk of these designs was discarded in favor of desired optimums, much has been learned in the process regarding the magnitude and characteristics of the subsystem interactions and their relative effect on the over-all craft performance. In addition to permitting optimization of craft performance based on range, payload, power requirements, and fuel economy, the program provides detailed data regarding the design requirements of the individual elements of the particular waterjet system under consideration. The computer program currently consists of 52 equations incorporating a total of more than 100 individual parameters. It is written in Fortran machine language and has been adapted to either the IBM 7090 computer or the Sperry-Rand UNIVAC computer. The program also incorporates an automatic plotting feature which provides a grid of thrust vs craft speed for any of the design schemes being analyzed. Details of the input and output parameters are included in the Appendix.

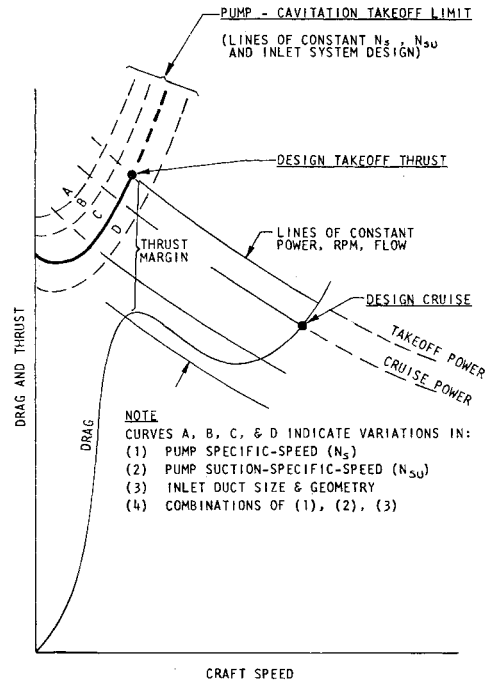

Fig. 6 Typical craft characteristics.

3. *Design trade example*

Figures 7–10 illustrate the usefulness of the computer program described in the preceding section and in the Appendix. They summarize typical data which form part of a design trade performed for a 300-ton, 50-knot hydrofoil with a fixed payload mission. The curves shown in the figures are only a representative sample of the selection criteria provided by the computer. As shown in the Appendix, the computer also provides comprehensive tabulation of additional waterjet design parameters which facilitate the final selection.

Figure 7 consists of curves for craft range, required cruise and takeoff power, and over-all propulsive efficiency as functions of design cruise jet-velocity ratios r_o. Each set of curves, designated A, B, and C, represent inlet system designs incorporating similar inlet system configurations categorized by the nominal areas of 600, 1050, and 1500 in.^{2}, respectively, and the associated total cruise drag. Several items are to be noted:

1) The peaks of the three range curves are all at a higher value of r_o than are the minima of the three corresponding cruise power curves. This situation indicates that a compromise must be made between maximum range and maximum speed if the available power level is fixed. In this connection, the fuel economy yardstick Y discussed in Sec. IIC3 also should be considered. Although for reasons of clarity they are not shown in Fig. 7, the fuel-economy curves peak for values of r_o which are intermediate between the peaks of the range curves and the minima of the cruise power curves. With these three sets of craft criteria, the designer

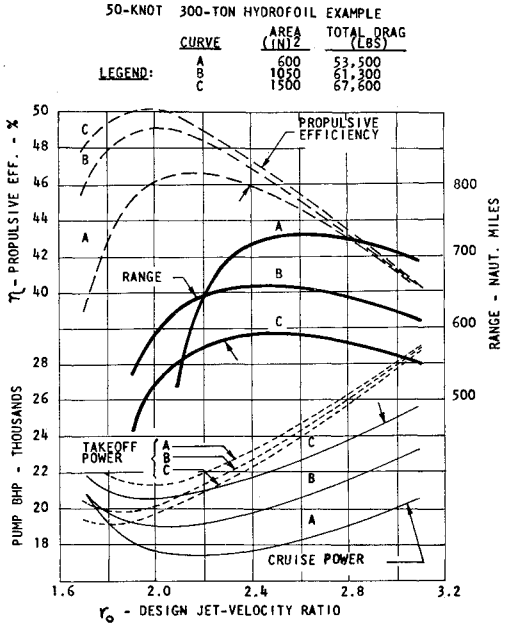

Fig. 7 Over-all waterjet criteria.

is provided essential tools for selecting the system which is best suited to the particular mission requirements.

2) Curve A, representing the minimum nominal inlet area, indicates the maximum range and the minimum cruise power (by reason of low weight fractions and low parasitic drag). On the other hand, curve A represents maximum required takeoff power (by reason of lowest takeoff efficiency resulting primarily from highest ratio of r_{to} to r_o). Again, additional tools are provided for the selection process compromises.

3) The spread between required cruise and takeoff power increases noticeably with increase in r_o. This characteristic feature of a waterjet system is particularly useful to the designer since the continuous and short-duration ratings of gas-turbine engines are usually defined within close limits since they have a direct bearing on operational life.

4) An additional comment is in regard to the propulsive-efficiency curves. Note that curve C (maximum area) represents maximum efficiency but requires maximum cruise power (by reason of high parasitic drag), and provides minimum craft range (by reason of high required power and high system weight fractions).

The discussion associated with Fig. 7 considers primarily the over-all craft criteria. However, the final system selection cannot be predicated on these alone, but must be tempered by the evaluation of subsystem parameters which may limit the range of practical selections. Figures 8–10 are included to identify certain subsystem characteristics for the chosen example.

Figures 8 and 9 represent variations in craft range, total drag, pump impeller specific speed N_s, and pump rpm, in terms of nominal inlet-area variations, for constant values of jet-velocity ratio r_o at the design foilborne condition. As noted, Fig. 8 is identified by $r_o = 2.1$, and Fig. 9 by $r_o = 2.5$. Of special interest in these figures are the N_s curves which indicate a marked variation in this parameter as the inlet area is varied. This information is of particular significance to the designer since N_s values (per impeller side) in the range of 1000 and below normally indicate a region where typical pump efficiencies decay rapidly. Another important subsystem parameter is pump rpm which requires evaluation based on speed-converter considerations. Assisted by the type of information provided in Figs. 7–9, the designer may find it feasible to select a system incorporating an existing speed-converter design, or ideally, he may select a configuration which, without too great a compromise, entirely eliminates this component.

Figure 10 provides waterjet weight data for the same two values of jet-velocity ratio, $r_o = 2.1$ and $r_o = 2.5$. The two A curves shown represent the waterjet-system craft-weight fractions minus prime-mover and speed-converter weights, but include the contained water in the entire system. The two B curves shown represent the weight fractions of the pumps plus the pump-contained water, a component item of curve A. These pump weights are calculated for the various craft designs identified by the variable inlet areas, each design incorporating a single pump rated at 30,000-BHP maximum. The pumps are all of the centrifugal-type incorporating twin, double-suction impellers in parallel which discharge separately through twin nozzles. The weight data are predicated on a comprehensive parametric study performed by a pump manufacturer on a wide range of specific speeds and sizes and are therefore considered realistic. The pertinent data here are twofold:

1) The curves show a significant variation of pump weight with a variation of r_o and duct size, for a constant power level.

2) The pump-plus-contained-water weight fraction range of 4 to 5% shown for $r_o = 2.5$ (curve B) is considered reasonable for hydrofoil application. It is noteworthy that these values result from the utilization of current state-of-the-art pump designs (noninducer types) with maximum suction-specific-speed characteristics of 12,000 per impeller side.

Also to be considered is the fact that pump weight is related to pump size, and a satisfactory over-all system weight fraction may not be a sufficient yardstick. The designer, therefore, must note the pump size data provided by the

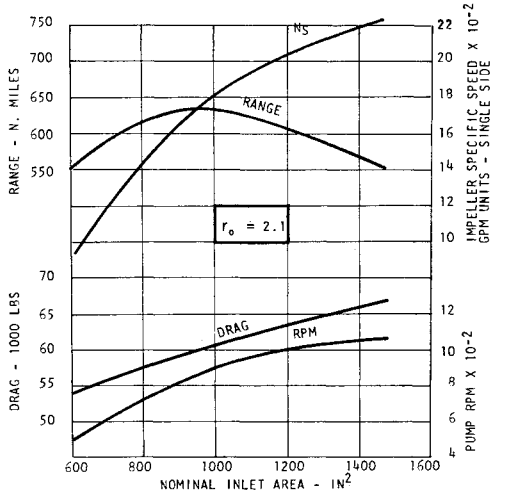

Fig. 8 Subsystem evaluation.

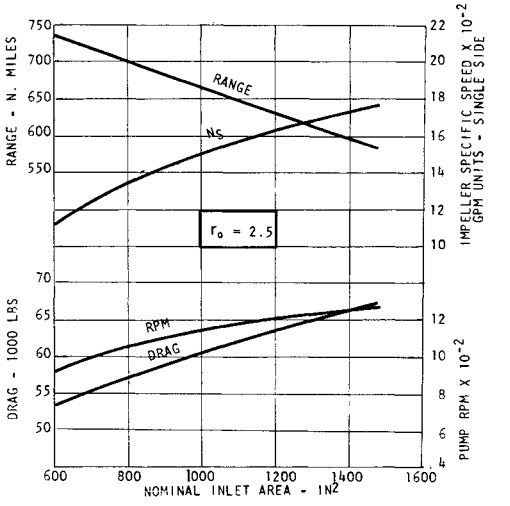

Fig. 9 Subsystem evaluation.

computer output to insure a satisfactory propulsion machinery arrangement for the selected system.

E. Waterjet Takeoff Performance

The takeoff performance of a waterjet system requires special attention since this is the operational mode that imposes the most severe requirements on the system. Both the power level and the cavitation resistance are pertinent: the power requirement is usually a maximum at the actual takeoff point, and the cavitation requirement is at a maximum throughout the takeoff mode transient. In contrast, after takeoff and throughout the foilborne mode, the waterjet-duct, static-pressure environment inhibits the occurrence of cavitation.

The selection of the jet-velocity ratio that satisfies the power required vs the prime-mover power available, both at cruise and takeoff, is made at the time of the computer-trade evaluation discussed earlier. However, adequate power will not insure sufficient takeoff thrust unless the pump and inlet system have been designed with adequate cavitation-resistance characteristics.

Ultimately, it is evidently the pump-cavitation performance which limits thrust when adequate power is available. However the pump-cavitation performance is not only a result of the pump characteristics, but it is also naturally a function of the available energy level (available *NPSH*) which is provided to the pump by the inlet system. The avilable *NPSH* can be calculated readily by the judicious use of existing experimental coefficients when the inlet system is conservatively sized to preclude the onset of cavitation in critical areas, such as between the scoop turning vanes. However, in the event parasitic (power-strut and inlet-pod) drag considerations impose severe requirements on the inlet-system sizing, the inlet-system cavitation characteristics will have an important effect on the *NPSH* delivered to the pump and, in turn, on the cavitation performance of the pump proper. Therefore, in order to achieve an integrated waterjet design that will meet the takeoff thrust requirements with minimum parasitic drag, it is essential to define the cavitation characteristics of both the pump and the inlet system. A brief discussion of the methods used to obtain these data is provided in the following subsections.

1. Pump evaluation

The pump cavitation resistance is usually defined by a parameter designated as suction specific speed (N_{su}). This parameter is related to the impeller specific speed (N_s) and to the critical cavitation sigma (σ_c) by the following expression:

$$N_s = N_{su} \cdot \sigma_c^{3/4} = \frac{(NPSH)_c^{3/4}}{(H_p)^{3/4}} \tag{17}$$

For conventional pump designs, the suction-specific-speed characteristics of a wide range of impeller types has been experimentally established by the pump manufacturers over a period of many years. From the manufacturer's N_{su} data, the energy level (*NPSH*) required at the pump inlet over the full range of operating conditions may be calculated readily. However, because of the complex nature of the cavitation phenomenon, acceptance texts performed on the particular pump procured are desirable to verify the manufacturer's guaranteed data.

For more recently developed configurations, such as those that incorporate inducer-type impellers and which are intended to operate beyond the incipience of cavitation, more care is required in evaluating a particular design. This is the case, since for this design concept, the effects of model scale on performance and operational life have not been resolved to date. Additional remarks regarding the significance of flows in a cavitating regime in relation to model scale are provided in the following section.

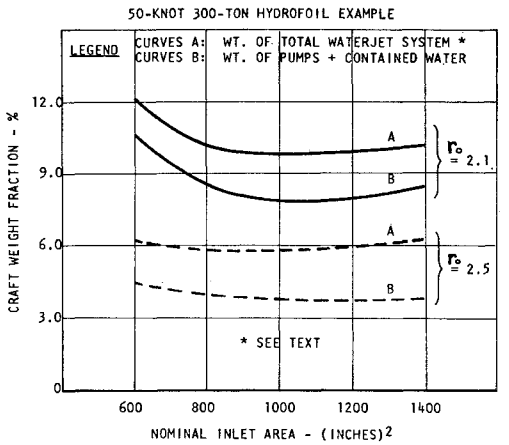

Fig. 10 Waterjet weight fractions.

2. Inlet system evaluation

As discussed in Sec. IIA, the inlet system consists of several distinct components. However, from a takeoff-mode cavitation consideration, the critical items are the inlet scoop and the connecting lower portion of the vertical duct where diffusion to the pump inlet section normally begins.

Since the function of the scoop is to capture efficiently the freestream flow under the full range of operating conditions, the most suitable design is evidently a compromise between the widely varying requirements during takeoff and cruise. During takeoff the inlet-to-freestream velocity ratio is high, the pressure levels in the scoop are low, and internal cavitation is the primary concern. During cruise, the inlet-to-freestream velocity ratio is relatively low, the pressure levels in the scoop are relatively high, and consequently the resistance to internal cavitation is high. However, for the cruise mode the susceptibility of external lip cavitation is a factor that also influences the design of the lip and pod contours.

The complexity of three-dimensional flow concepts in a vaned-scoop configuration is greatly compounded by the susceptibility to cavity formation, and the associated implications of flow distribution and energy dissipation. Analytical methods alone, therefore, are not considered sufficient, but must be predicated on reliable, large-scale-model data which reflect the minimum "scale effects." This latter requirement is considered important since little information is currently available regarding the effect of scale associated with flows in a cavitating environment.

In order to characterize the internal cavitation resistance of a particular inlet system design, the Boeing Company has made full use of the technology developed over many years by the hydroelectric turbine industry. This technology has been developed in order to determine the incipient cavitation characteristics of very large turbine wheels from the results of scale-model testing in the laboratory.

This concept consists essentially of determining the "break" in a nondimensional parameter designated the "plant sigma" or more recently the "cavitation index." This index first proposed by Thoma[4] in 1924 is defined as

$$\sigma_i = \Delta H/H \tag{18}$$

The cavitation index is plotted against a convenient parameter which is a measure of the system performance, such as efficiency (in the case of hydraulic rotating machinery) or any other measure of energy loss. Each curve represents conditions where the model flow kinematics are held constant

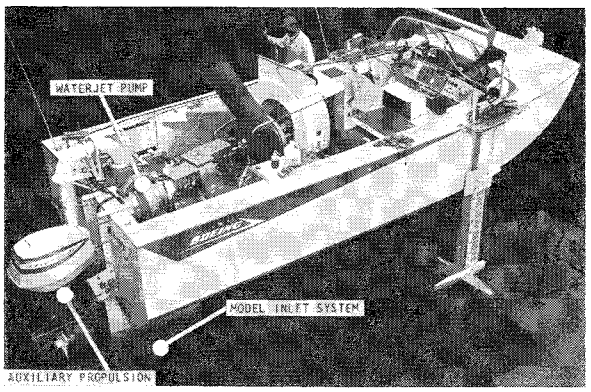

Fig. 11 Boeing dynamic test platform.

while the cavitation index is varied, usually by controlling the numerator of the index ratio. The break in the curve represents the "critical" sigma, and it is the desired indication that a cavity in the critical region of the flow has affected the performance of the system. The critical sigma thus obtained is therefore also the pressure-drop coefficient which characterizes the cavitation resistance of the system for a given pattern of flow angles.

In the application of the existing cavitation technology to the inlet scoop of a waterjet system, an important consideration regarding cavity "scaling" evolved. A turbine wheel or pump impeller normally will reflect a change in performance as soon as a measurable cavity forms in the flow path. In this case, therefore, the incipient point of cavity formation is the critical sigma desired and this is obtained readily by the use of relatively small-scale models. This is possible in the foregoing application since the full-scale units are rated at a sigma index value higher than the critical sigma, and "cavity scaling" is not required. The validity of the model data has been proven by the results of numerous field tests (some of these personally conducted by one of the co-authors), which have shown remarkable agreement with the model predictions.

The inlet scoop during takeoff presents a more difficult situation in that a lip cavity usually forms very early in the takeoff mode. When the scoop lip cavity first forms it tends to be small and stable, and measurements have indicated excellent recovery downstream. Such a lip cavity evidently will not trigger a sudden change in the over-all inlet-system performance until it grows to a size which is large enough to become unstable or to cause energy to be dissipated downstream. In this particular application of cavitation testing, therefore, stable and discrete cavities exist in the flow regime which is required to be scaled to full size performance; and it is consequently essential to simulate the flow, not only to the incipient point, as described for hydraulic machinery testing, but also to simulate the size and characteristics of the cavity beyond its inception.

The complex technology required for accurate cavity scaling, although under intense study for some years, is not within the current state of knowledge. In addition, aside from the scale factor, it has been shown that the nuclei content of the liquid will affect the incipience of cavity formation and that the gas content (dissolved and free) has a bearing on the size and characteristics of the cavity. Because of the preceding factors, experimental data of this nature should be obtained from large-scale models in a realistic fluid environment in order to obtain initial design parameters or to verify design conclusions obtained by other experimental methods.

In order to satisfy the stringent requirements discussed previously with regard to the reliable evaluation of an inlet-scoop performance, the Boeing Company has recently developed a dynamic testing platform and testing techniques which already have furnished much valuable information. This capability provides the design engineer with well-defined sigma-break curves measured on a large-scale model (currently one-half scale) in an actual seawater environment over the full range of the takeoff mode. In addition, this system has the capability of obtaining photographs of the inlet-pod external flow up to speeds in the region of 50 knots.

Figure 11 is a photograph of the dynamic test platform being lowered into the water. This facility consists of a 3-ton, 500-hp, waterjet-propelled hydrofoil craft "Little Squirt," with auxiliary propulsion provided by a 100-hp outboard engine. The main engine is a Boeing gas turbine which drives a 3500 gal/min, 450-ft-head centrifugal pump through a speed converter. The outlet nozzle is interchangeable, provisions having been made for implementing either a fixed- or variable-area nozzle. The model data are recorded automatically by means of a transducer-oscillograph system and are also constantly monitored visually, and manually recorded by a redundant system of indicating gages. The ability to monitor visually the test data is a key function, as explained below. The heave attitude of the craft is measured by means of a sonic transmitting and receiving system; the ditch and roll attitude by use of a gyroscopic, stable platform. In this figure, the model consists of a one-half-scale inlet scoop and pod, and a vertical diffusing duct which is within the rear power-strut-foil assembly of the craft. The inlet-system model, consequently, is an integral part of the craft propulsion system, but the model performance is isolated from the rest of the system by means of piezometer taps and flow measurements.

As explained earlier, the purpose of this type of test is to obtain the "break" in individual cavitation index curves while the flow kinematics are maintained constant. On Little Squirt, the index is varied primarily by varying the denominator of the index ratio, i.e., the flow rate through the system. However, in order to maintain the inlet flow angles constant, the platform speed must be varied in the same proportion as the desired variation in flow rate. This requirement is accomplished readily by varying the output of the 100-hp auxiliary engine while monitoring the flow rate and boat speed by the means of calibrated indicating gages. As may be seen in the photograph, these gages are mounted on the pilot instrument panel and are sufficiently large to facilitate accurate settings to obtain reliable "on condition" data recording.

The series of tests associated with the model shown in the photograph is currently in progress, and the technique has been proved. It is considered that the results currently being obtained will have a major influence on the design of waterjet-propelled hydrofoils.

III. Conclusions

Waterjet-propelled hydrofoils present to the designer a wide spectrum of alternative subsystem selections which can be evaluated properly only by comparing the performance of the integrated whole. The recommended digital computer technique for selection of the waterjet design makes the rigorous (vs oversimplified) analyses of complex component interactions possible.

It is shown by specific examples that, through the recommended approach and the use of state-of-the-art pumps with proved design features, power requirements and total waterjet-system weight fractions can be maintained at reasonable levels. Although continued developmental effort is essential to advance the existing waterjet-propulsion technology, particularly in the areas of pumps and inlets, a first-generation, waterjet-propelled hydrofoil is currently under construction by the Boeing Company. This craft therefore will provide the means to demonstrate the desirability of waterjet propulsion for hydrofoils, and the soundness of the recommended concepts.

IV. Appendix

A. Program Input Parameters

The following information is provided to the computer for each hydrofoil configuration to be evaluated:

Over-all craft parameters

1) Payload (for a calculated range) or range (for a calculated payload)
2) Design-cruise speed
3) Takeoff speed at drag hump
4) Design-cruise drag
5) Takeoff-hump drag
6) Craft gross weight
7) Craft "fixed" weight (i.e., the weight of craft components not affected by variation in the propulsion system configuration). The difference between 6 and 7 is therefore constant for a given mission, and is the sum of all weights attributable to the propulsion system, plus the propulsion fuel-load weight.
8) Prime-mover maximum continuous power level
9) Prime-mover, maximum short-duration power level
10) Prime-mover specific fuel consumption

Pump parameters

11) Pump efficiency at design point
12) Pump suction specific speed at design point (cavitation resistance parameter)
13) Barometric pressure less water-vapor pressure
14) Pump dry-weight coefficients vs pump impeller specific speed (tabular data)
15) Pump contained-water weight coefficients vs pump impeller specific speed (tabular data)
16) Total number of pump impellers (in parallel)
17) Total number of impeller stages (in series)
18) Single or double suction impellers
19) Elevation of pump centerline above water surface, foilborne
20) Elevation of pump centerline above water surface, hullborne

Inlet system parameters

21) Length of inlet-duct system (total)
22) Length of inlet-duct system above the flying waterline (for weight calculations)
23) Area of scoop inlet
24) Area of scoop outlet
25) Area of inlet-duct outlet (at pump)
26) "Effective" area of inlet duct (for skin loss calculations)
27) "Effective" hydraulic radius of inlet duct (for skin loss calculations)
28) Average area of inlet duct above the flying waterline (for weight calculations)
29) Inlet-scoop loss coefficient
30) Inlet-strut loss coefficient
31) Upper-turn, inlet-duct, loss coefficient
32) Capture-area-to-scoop-inlet loss coefficient
33) Inlet-duct skin-roughness parameter
34) Number of inlet ducts
35) Density of water in inlet duct
36) Submergence of inlet scoop during takeoff
37) Inlet-scoop-turn, pressure-gradient coefficient
38) Inlet-scoop, energy-loss coefficient

Outlet system parameters

39) Length of outlet-duct system (for loss calculations)
40) Length of outlet-duct system (for weight calculations)
41) "Effective" area of outlet duct (for loss calculations)
42) Average area of outlet duct (for weight calculations)
43) Average density of outlet duct plus contained water
44) Number of outlet ducts
45) Outlet-duct, skin-roughness parameter
46) Outlet-duct loss coefficient
47) Outlet-nozzle loss coefficient
48) Elevation of nozzle centerline above water surface, foilborne
49) Elevation of nozzle centerline above water surface, hullborne

B. Program Output Parameters

The following information is provided by the computer for each configuration under study.

Over-all craft parameters

1) Range (for a given mission payload, or payload for a given mission range)
2) Payload ton-miles per ton of fuel consumed
3) Required power at the design-cruise speed
4) Required power at the takeoff-drag hump with the specified thrust-over-drag margin
5) Cruise speed at the maximum continuous power level specified (see input)
6) Thrust-over-drag margin at the maximum short-duration power level specified (see input)
7) A complete grid of net propulsion thrust vs craft speed for a family of power and rpm levels. This grid covers the hullborne and foilborne modes and is provided by the computer in tabular and graph form. The pump cavitation thrust limit is also shown on the grid.
8) Propulsive efficiency at design cruise
9) Jet-velocity ratio at design cruise
10) Propulsion fuel load required
11) Total weight of waterjet-subsystem components

Pump parameters

12) Discharge per pump impeller at design point
13) Head rise per pump impeller at design point
14) Pump impeller specific speed at design point
15) Pump impeller diameter
16) Pump rpm at design point
17) Required pump *NPSH* at design point and design rpm
18) Required pump *NPSH* at design point and takeoff-hump rpm
19) Pump rpm ratio at the takeoff hump
20) Pump rpm ratio at the short-duration maximum power level
21) Pump dry-weight coefficient
22) Pump contained-water-weight coefficient
23) Pump dry weight
24) Pump contained-water weight
25) Weight of pumps plus contained water per maximum brake horsepower required
26) Specific-speed ratio

Inlet system parameters

27) Inlet-to-freestream velocity ratio at design cruise
28) Inlet-to-freestream velocity ratio at the takeoff-drag hump
29) Velocity ratio at scoop outlet
30) Velocity ratio at strut outlet
31) Velocity ratio at "effective" strut section (for skin-friction calculation)

32) Over-all loss coefficient
33) Darcy-Weisbach skin-friction coefficient (for given skin roughness and duct size)
34) Inlet-scoop cavitation margin at the takeoff-drag-hump, specified thrust condition

Outlet system parameters

35) "Equivalent" hydraulic radius (for skin-friction calculations)
36) Darcy-Weisbach skin-friction coefficient (for given skin roughness and duct size)
37) Velocity ratio at the "equivalent" section
38) Over-all loss coefficient (including elevation head loss)
39) Weight of outlet duct plus contained water in inlet and outlet systems above flying water line

References

[1] Levy, J., "The design of water-jet propulsion systems for hydrofoil craft," Soc. Naval Architects Marine Engrs., Marine Technology **2**,15–25, 41 (January 1965).

[2] Johnson, V. E., Jr., "Waterjet propulsion for high speed hydrofoil craft," AIAA Paper 64-306 (1964).

[3] Traksel, J. and Beck, W. E., "Waterjet propulsion for marine vehicles," AIAA Paper 65-245 (1965).

[4] Thoma, D., "Experimental research in the field of water power," *Transactions of First World Power Conference, London, Vol. 2: Water Power Production, Preparation of Fuels, Steam Power Production* (Percy, Lund, and Humphries, London, 1925), pp. 536–551.

JULY 1967 J. HYDRONAUTICS VOL. 1, NO. 1

Pressure Hulls for Deep-Submergence Vehicles

HAROLD BERNSTEIN*
Deep Submergence Systems Project, Department of the Navy, Chevy Chase, Md.

Deep-submergence vehicles should be small, highly maneuverable, and have high payload capacity. To attain these objectives, the pressure hulls for the vehicles must be the lightest possible structures that can withstand the pressures at operating depths. The efficiency of materials used in pressure hulls is expressed in terms of weight/displacement for a particular structure. Therefore, light, strong materials are at a premium. In addition, hull materials must be state-of-the-art, and stable in the marine environment. For moderate depths of about 6000 ft, tough, fail-safe metals such as HY 140 steel appear satisfactory. To achieve intermediate depth capabilities to 12,000 ft, higher strength metals such as the 18% nickel maraging steel or the titanium-6% aluminum 2½% molybdenum are required. Some of these materials cannot meet the charpy impact or drop weight tear test criteria. For these materials, other toughness approaches, such as fracture mechanics, must be utilized. For the great depths, down to 20,000 ft, high-strength steels or titanium alloys, or nonmetallics such as glass, either in the solid or fiber form, can be utilized. To insure reliability with the latter materials, it will be necessary to develop proof-testing procedures. Two types of vehicles are planned for the Deep Submergence Systems Project—a 6000 ft rescue vehicle and a 20,000-ft search vehicle, to be operable by 1968 and 1970, respectively. The pressure hull for the 6000-ft rescue prototype will be fabricated from HY 140 steel. Advanced material technology will be required for the 20,000-ft pressure hull. The present concept calls for a manned metal capsule with buoyancy supplied by simple floatation spheres of glass or ceramics.

THE great depths of the ocean have been penetrated by large, relatively immobile submersibles known as bathyscaphs. In 1960, Trieste I reached the floor of the Challenger Deep, 35,800 ft down. To explore the depths fully, submersibles must have, in addition to depth capability, the mobility to explore and survey extended areas at a reasonable speed and the ability to perform useful work on the ocean bottom. It is intended that the new submersibles have these characteristics.

The bathyscaph is heavy and cumbersome because of its large buoyancy chamber. Trieste II carries 47,000 gal of gasoline in its float tanks. Since the compressibility of gasoline is significantly greater than that of seawater, a large amount of expendable ballast must be carried to maintain neutral buoyancy. For each 3000 ft of dive, 2000 lb of shot must be dropped. The over-all displacement of Trieste II is 220 tons.

Presented as Paper 66-696 at the AIAA/USN 2nd Marine Systems & ASW Conference, Los Angeles—Long Beach, Calif., August 8–10, 1966; submitted August 4, 1966; revision received December 28, 1966. [6.09, 6.14]

* Materials and Structures Engineer, Vehicle Branch.

The pressure hull of Trieste II is a 7-ft-diam steel sphere that is heavier than the water it displaces by a factor of 2. The principal function of the pressure hull in the Trieste is to provide hotel space for the crew and control equipment. The vehicle size may be reduced considerably if the pressure hull, in addition to hotel space, provides buoyancy. Alvin is an example of the latter type of vehicle. The pressure hull of Alvin is a 7-ft steel sphere that displaces about 1.4 times its own weight of water and contributes substantially to the buoyancy requirements of the vehicle. The Alvin displaces about 15 tons over-all. It is a relatively shallow vehicle, with a 6000-ft operating depth, but it is hoped that the buoyant hull principle can be extended to great depths.

Consideration of power requirements, maneuverability, and surface support lends weight to the desirability of small, deep submersibles. In addition, mission constraints may impose limitations upon vehicle size and weight. In the Deep Submergence Systems Project, there is a requirement for a rescue vehicle that can be transported in a C141 aircraft. Hence, the following vehicle characteristics were established: size: 44 ft long, 8-ft diam; weight: approx. 25 tons in air; depth: 6000 ft; speed: 5 knots max, 3 knots for 12 hr; personnel: